AD-A022 985

IONOSPHERIC CORRECTION USING TWO-FREQUENCY
MEASUREMENTS

T. M. Pass

Massachusetts Institute of Technology

17 SEP 1971

Project Report	PPP-112
Ionospheric Correction Using Two-Frequency Measurements	T. M. Pass 25 August 1971

Lincoln Laboratory

MASSACHUSETTS INSTITUTE OF TECHNOLOGY

Lexington, Massachusetts

D D C
RECEIVED
APR 9 1976

Unclassified

Unclassified

MASSACHUSETTS INSTITUTE OF TECHNOLOGY

LINCOLN LABORATORY

IONOSPHERIC CORRECTION
USING TWO-FREQUENCY MEASUREMENTS

T. M. PASS

Group 35

PROJECT REPORT PPP-112

25 AUGUST 1971

LEXINGTON   MASSACHUSETTS

Unclassified

Unclassified

ii

Unclassified

I. INTRODUCTION

The purpose of this report is to present a number of results regarding errors in radar measurements produced by propagation through the ionosphere. The emphasis is on the dependence of these errors on radar frequency, and on the possibility of determining and removing the errors by making simultaneous measurements at two radar frequencies.

The application which motivates this collection of results is primarily to data taken by the ALTAIR radar, which operates simultaneously at VHF and UHF frequencies. For these frequencies, and particularly at VHF, errors in metric data induced by the ionosphere are often large in comparison with errors from all other sources. Thus the degradation of metric data caused by propagation through the ionosphere is significant, and the measurement of this error is highly desirable.

The use of two-frequency measurements to determine ionospheric corrections is by now a well-established technique,[1] but until recently these methods have not been applied routinely to data from the KREMS radars. Efforts toward correcting the metric data have focused primarily on computing the correction using model ionospheres and ray-tracing calculations.[2] It is the purpose of this report to show the feasibility of determining these corrections by direct measurement using current ALTAIR capabilities. The techniques are currently being used in post-mission analyses with gratifying success.

The ionospheric effects discussed here are those on radar range, elevation angle, coherent doppler velocity, pulse shape, and wave polarization. With the exception of the elevation correction, these results are well known. They are presented for convenience, and in order to cast them into a form which demonstrates their applicability to ALTAIR data. Corrections of the

1

azimuthal angle, effects due to ionospheric disturbances, and tropospheric refraction are not considered here.

2. RANGE ERROR

The apparent range R of a body from the radar, as measured by time delay, is:

$$R = c\int_p ds/v_g$$

where v_g is the group velocity and the subscript p indicates that the integral is one-way over the ray path.

For ionospheric propagation, $v_g = cn$, where n is the refractive index. If the effect of the earth's magnetic field and electron collisions can be ignored, n is given by

$$n^2 = 1 - 2X$$

with

$$X = 40.2N/f^2$$

where N is electron density in m^{-3} and f is radar frequency in Hz. For VHF frequencies or higher, $X \ll 1$ and terms of order X^2 can be ignored. Thus

$$R = \int_p \frac{ds}{n} \approx \int_p ds(1 + X)$$

The effect of path curvature on apparent range can be shown to be $O(X^2)$ so that $\int_p ds \approx R_t$, the true range, and

$$\Delta R = R - R_t = \int_p ds X(s) \tag{1}$$

is the range error. Rewrite R as

$$R = R_t + B/f^2 \tag{2a}$$

where

$$B = 40.2 \int ds N(s) \tag{2b}$$

If R is measured at two different radar frequencies f_1 and f_2, the measured ranges differ by

$$\Delta R_{12} = R_1 - R_2 = B(f_1^{-2} - f_2^{-2})$$

also

$$\Delta R_1 = R_1 - R_t = B f_1^{-2}$$

Eliminating B:

$$R_1 - R_t = g \cdot (R_2 - R_1) \tag{3}$$

where

$$g = [f_1/f_2)^2 - 1]^{-1} \tag{4}$$

Thus the range difference ΔR_{12} can be used to find the range error ΔR_1, the true range R_t, and the apparent range at any other frequency f_3. In particular, for ALTAIR we can set $f_1 = 415 \times 10^6$, $f_2 = 155.5 \times 10^6$, giving $g = 0.16333$. Using this value in (3) with the UHF - VHF range difference gives the UHF range error and also VHF error.

3. PULSE BROADENING

Once the range error is computed by two-frequency measurement, the amount of spreading of either pulse due to ionospheric dispersion can be found, provided that the undispersed pulse shape is known. If S(t) is a chirped pulse, and

$$\tilde{S}(\omega) = \int_{-\infty}^{\infty} dt\ S(t) e^{-i\omega t}$$

is its fourier transform, then the signal received by the radar can be written as

$$A(t) = \int_{-\infty}^{\infty} \frac{d\omega}{2\pi} e^{i\omega t}\ \tilde{S}(\omega)\ P(\omega) \tilde{S}^*(\omega)\ W(\omega) \tag{5}$$

where

$$P(\omega) = e^{-2i\frac{\omega}{c}\int_0^R n(s)\,ds}$$

3

is the transfer function for propagation through the ionosphere.
Here $\tilde{S}^*(\omega)$, the complex conjugate of $\tilde{S}$, is the matched filter,
and $W(\omega)$ is any additional weighting applied to reduce sidelobes.

Expression (5) can also be written as

$$A(t) = \int_{-\infty}^{\infty} \frac{d\omega}{2\pi} e^{i\omega t} \tilde{A}_o(\omega) P(\omega)$$

where
$\tilde{A}_o(\omega) = \tilde{S}(\omega)^2 W(\omega)$ is the transform of the compressed
pulse. Expanding the refractive index n as before:

$$A(t) = \int_{-\infty}^{\infty} \frac{d\omega}{2\pi} e^{i\omega(t - \frac{2R}{c})} A_o(\omega) e^{i \frac{E}{\omega c}} \tag{6}$$

with $E = 8\pi^2 B$.

The spectrum $\tilde{A}_o(\omega)$ is a peak located at the radar angular
frequency ω_o, so that $\tilde{A}_o(\omega) = A_1(u)$ with $u = \omega - \omega_o$, and

$$A(t) = e^{i\omega_o t} + \int_{-\infty}^{\infty} \frac{du}{2\pi} A_1(u) e^{i[ut_- + u^2 \frac{E}{\omega_o^3 c}]} \tag{7}$$

with

$$t_\pm = t - \frac{2R}{c} \pm \frac{E}{\omega_o^2 c}$$

Here we have expanded ω^{-1} in powers of u and retained $O(u^2)$.

If the compressed undispersed pulse $A_o(t)$ is approximated
by a Gaussian:

$$A_o(t) \propto e^{i\omega_o t} e^{-\left[\frac{t}{2\tau}\right]^2} \tag{8a}$$

then

$$A_1(u) \propto e^{-(\tau u)^2} \tag{8b}$$

Inserting this form in (7), we find

$$A(t) \propto e^{i\omega_o t} + (a^2 - i\epsilon)^{-\frac{1}{2}} e^{-\frac{(\omega_o t_-)^2}{4(a^2 - i\epsilon)}} \tag{9}$$

with

$$a = \omega_o\tau \quad \text{and} \quad \epsilon = E/(\omega_o c).$$

4

The pulse shape in terms of radar cross section is proportional to

$$|A(t)|^2 \propto (a^4 + \epsilon^2)^{-\frac{1}{2}} \, e^{-\left\{ \frac{(\omega_0 t_-)^2}{2} \frac{a^2}{a^4 + \epsilon^2} \right\}} \tag{10}$$

From this it follows that the effect of ionospheric dispersion is to increase the width and decrease the peak height by a factor

$$F = [1 + \gamma^2]^{\frac{1}{2}} \tag{11}$$

with $\gamma = \epsilon/a^2 = \frac{2}{\omega_0 c \tau^2} \triangle R$. For a given frequency ω_0 and compressed pulse width τ, the factor $F(\triangle R)$ determines the shape of the dispersed pulse. For ALTAIR VHF, $f_0 = 155.5$ MHz and a 3db width of 0.195μsec results in $\tau \approx 0.083 \mu$sec and $\gamma_v = 0.986 \triangle R_v$, where $\triangle R_v$ is VHF range error in kilometers. For UHF, $f_0 = 415$ MHz and a 3db width of 0.1μs implies $\tau \approx 0.042 \mu$s and $\gamma_u = 1.42 \triangle R_u$ with $\triangle R_u$ the UHF range error in kilometers. Thus, a measured $\triangle R_{uv}$ range difference of 2 km corresponds to a spreading factor $F = 2.5$ at VHF, and $F = 1.05$ at UHF. Since 2 km is a fairly typical range difference observed in tracking bodies above the peak of the ionosphere, it can be concluded that at these target heights the VHF pulse will often be broadened by a factor of two or more, while the dispersive effect on the UHF pulse is negligible.

The question remains as to whether the Gaussian approximation of the compressed pulse is a good one. Figure 1 shows a measured VHF long chirp compressed pulse shape, together with a fitted Gaussian. The pulse shape data are from the test ALTO 319B1 of 31 March 1971. The data points were generated by performing a range scan on a calibration sphere. The gaussian was fit by eye to the data points, which determined the value of τ given above. The measured pulse is seen to be slightly skewed
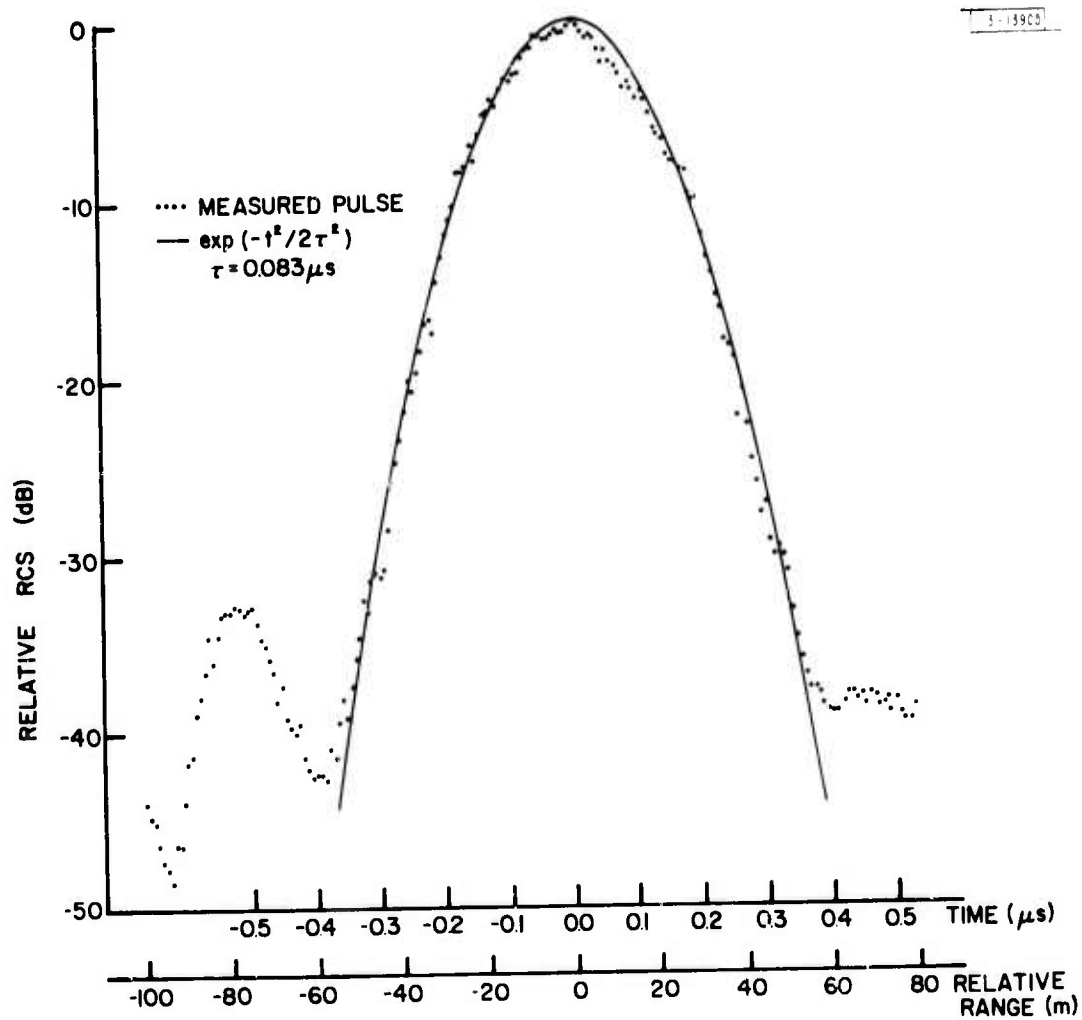
5

Fig. 1. ALTAIR VHF pulse and fitted gaussian.

6

at the top of the leading edge, but over most of the main lobe the agreement is very good.

If greater accuracy than that provided by the Gaussian fit is required, pulse shape dispersion can be computed without approximation. This is done by calculating numerically the convolution integral of the measured pulse shape with the time transform of the propagation factor. However, the reasonably good fit by the Gaussian spectrum indicates that the factor F given by (11) provides a sufficiently accurate measure of the pulse broadening.

The pulse spreading has significance for both radar cross section (RCS) and range measurements. If the VHF RCS of a hard body is measured as the return from the peak of the pulse, then the measured RCS will be too low by a factor of F. With RCS in dbsm, the error is

$$\Delta\sigma_{db} = -10 \log_{10} F \tag{12}$$

From the numerical estimates above, it follows that pulse spreading can cause errors in measured RCS as large as 5db at VHF.

Similarly the range resolution of the VHF pulse is taken to be the 3db width of 29m, as in Figure 1. The effect of propagation through the ionosphere is to multiply this number by F and thus degrade the resolution by this factor. The effect should be taken into account when measurements depending on the resolution length are analyzed.

One example of this dependence is the measured RCS of chaff clouds. Although pulse spreading causes the RCS of an individual dipole to decrease according to (12), the range resolution cell increases in length by a factor of F, so that on the average, F times as many dipoles contribute to the return. Thus except for very sparse chaff clouds (less than one dipole per resolution cell) and except for positions near the edge of the cloud, the average

7

chaff RCS should be unaffected by the pulse broadening. Since the RCS of a hard body immersed in chaff is decreased by (12), the signal-to-noise ratio (S/N) of body to chaff RCS is also decreased by an amount (12). Therefore the pulse spreading can cause losses of 5db in S/N when searching at VHF for a hard body in a chaff cloud.

4. ELEVATION ERROR

A. Flat Ionosphere Approximation

Once ΔR is known for a given radar frequency $f > 100$ MHz, the error in elevation angle can be computed without ray-tracing. To see this, consider first a flat ionosphere with electron density $N(h)$ a function of height only.

Referring to Figure 2, E_0 is the apparent elevation, τ the true elevation, and $\delta = E_0 - \tau$ is the elevation error. The ground range x_t can be represented in two ways:

$$x_t = R_t \cos \tau = \int_p dx = \int_p ds \cos E(h) \qquad (13)$$

Snells' Law is

$$n \cos E = \text{const.}$$
$$= \cos E_0$$

since $N(h)$ is assumed to vanish at the radar ($N(0) = 0$). Combining these two expressions:

$$R_t \frac{\cos \tau}{\cos E_0} = \int_p ds/n$$
$$= R \text{ (the apparent range)}$$

If the error δ is small, we can write

$$\cos \tau = \cos(E_0 - \delta) \approx \cos E_0 + \delta \sin E_0$$

so that

$$1 + \delta \tan E_0 = \frac{R}{R_t}$$

8
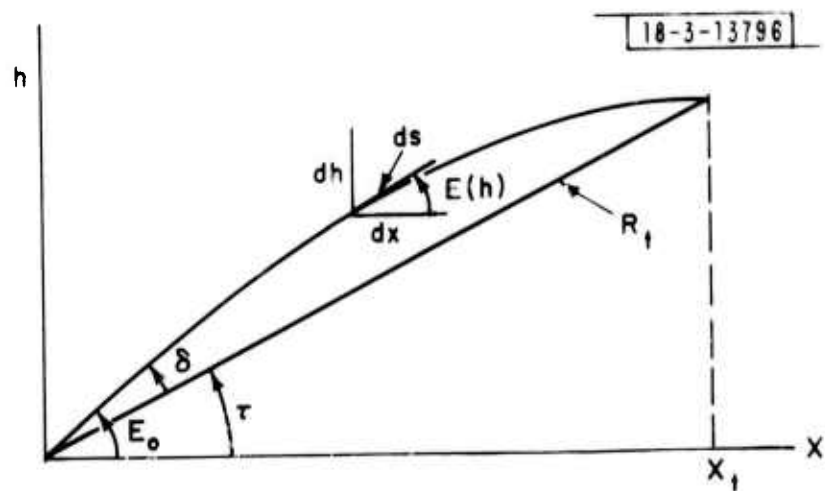
Fig. 2.   Propagation path for flat ionosphere.
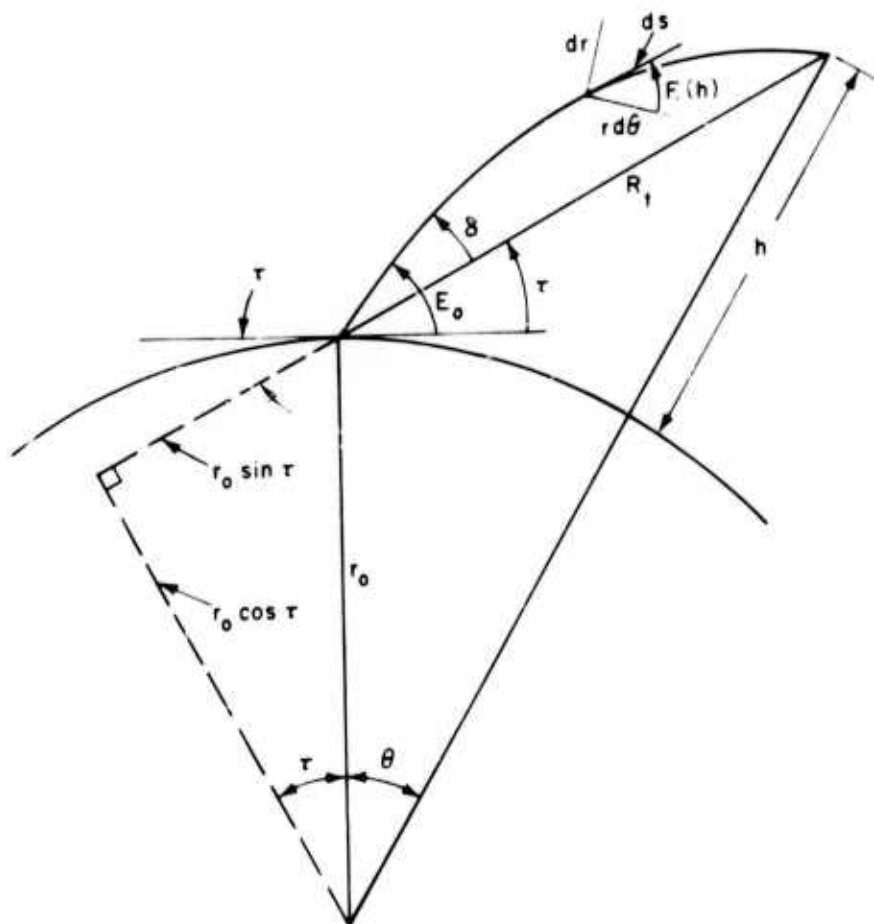
Fig. 3. Propagation path for spherical ionosphere.

or

$$\delta = \cot E_o \ \frac{\Delta R}{R} \qquad\qquad (14)$$

where we have replaced R_t by R in the last expression, introducing an error of order X^2. Equation (14) allows one to find the true elevation, given only the measured range and elevation, and the range error. It is valid to the extent that the earth can be thought of as flat, and assuming δ is small. In particular, the approximation of cos τ requires $\delta \ll 1$ and $\delta \ll 2 \tan E_o$. For radar frequencies $f > 150$ MHz and $E_o > 1^o$, these inequalities are virtually always satisfied.

Equation (14) was checked against the results of ray-tracing computation of δ. A re-entry trajectory and density profile $N(h)$ were chosen arbitrarily, and the ray-tracing program computed the corrections ΔR and δ for $f = 155.5$ MHz. The computed δ's agreed with (14) to within about 30% during later portions of the trajectory ($R < 1000$km), within about 50% at 2000 km range and within a factor of 2 at 2750 km. It is therefore desirable to recalculate (14) for the spherical case.

B. Spherical Case

Referring to Figure 3, the differential elements are related by

$$rd\theta \ = \ ds \cos E(h)$$

$$dr \ = \ ds \sin E(h)$$

Snell's Law for the spherical case is

$$nr \cos E = r_o \cos E_o$$

Using these relationships we can again construct an identity from which δ can be computed. Instead of ground range, it is more convenient in this case to use the geocentric angle θ:

11

$$\theta = \int_0^\theta d\theta = \int_p ds \, \frac{\cos E}{r} = \int_{r_0}^r dr \, \frac{\cot E}{r} \qquad (15a)$$

$$= \int_{r_0}^r \frac{dr}{r} \left\{ \left(\frac{nr}{r_0 \cos E_0} \right)^2 - 1 \right\}^{-\frac{1}{2}}$$

where r_0 is the earth radius. The angle θ can also be expressed as

$$\theta = \tan^{-1} \left\{ \frac{R_t + r_0 \sin \tau}{r_0 \cos \tau} \right\} - \tau \qquad (15b)$$

We then proceed as in the flat case, equating these two expressions for θ, expanding and keeping terms of first order in X and in δ. The result is

$$\delta = \cot E_0 \ (1 + \delta) \int_0^1 du \, \frac{X(u)}{(1 + \beta u)^2} \qquad (16a)$$

$$\Delta R = R \int_0^1 du X(u) \qquad (16b)$$

where

$$\beta = \frac{R}{r_0 \sin E_0}$$

and

$$u = S/R$$

Here S is the length along the straight-line path to the body being tracked. Equation (16b) is equivalent to (1), since the path difference introduces an error of order X^2.

C. The Sharp Ionosphere Approximation

In order to again express δ in terms of ΔR, we assume as a first approximation that the ionosphere is sharply peaked at a height H. corresponding to a value $u = u_p$. Then X(u) is essentially a δ-function, and we have

$$\delta \approx \cot E_0 \; \frac{1 + \beta}{(1 + \beta u_p)^2} \; \int_0^1 du \; X(u)$$

$$= \; \frac{1 + \beta}{(1 + \beta u_p)^2} \; \cot E_0 \; \frac{\Delta R}{R} \tag{17}$$

where

$$(1 + \beta u_p)^2 = 1 + \frac{H(2r_0 + H)}{r_0^2 \sin^2 E_0} \tag{18}$$

Equation (18) defines u_p as long as the body is above the height H, i.e. for $u_p < 1$. For lower altitudes we can set $u_p = 1$ in (17).

Equation (17) reduces to (14) as $\beta \to 0$, showing that the flat-earth result (14) is valid for $R \ll r_0 \sin E_0$.

In the opposite limit, $R \gg r_0 \sin E_0$, (17) reduces to

$$\delta \approx \frac{\cos E_0}{2H} \; \cdot \; \Delta R$$

This approximation holds early in an observed re-entry, when E_0 is small and R is large. In this case, $\cos E_0 \approx 1$, and if we arbitrarily choose an effective height H = 400 km for the ionosphere, we arrive at

$$\delta_{mr} \approx 1.25 \; \cdot \; \Delta R_{km}$$

where δ is in milliradians and ΔR is in kilometers. This explains the rough equivalence between δ and ΔR which has been observed in comparing ALTAIR and ALCOR metric data from simultaneous tracks on the same target. The fact that the equivalence does not always hold is also explained, since it is only valid for $R \gg r_0 \sin E_0$.

Equation (17) was tested against the ray-tracing program using a re-entry trajectory, a satellite trajectory, and several ionospheric profiles in various arbitrary combinations. It was found that with a proper choice of H, δ agreed with the ray-

tracing result to within 2 or 3% for body altitudes sufficiently higher than H (about 100km higher). At lower altitudes, the agreement typically worsened to 10 to 15%. To improve this situation it is necessary to include the effect of non-zero width of the ionospheric peak.

D. The Gaussian Ionosphere Approximation

A rough model of the peak is a Gaussian:

$$N(h) = N_o e^{-\left\{\frac{h - H}{\sigma_h}\right\}^2}$$

which translates near the peak to

$$X(u) = X_o e^{-\left\{\frac{u - u_p}{\sigma}\right\}^2}$$

with

$$\sigma = \sigma_h / \left| R \sin E_o (1 + \beta u_p \cos^2 E_o) \right| \tag{19}$$

Using this $X(u)$ in (16a), expanding and keeping terms of first order in σ:

$$\delta = \cot E_o \frac{\Delta R}{R} \frac{1 + \beta}{(1 + \beta u_p)^2} \left\{ 1 + \frac{\beta \sigma}{1 + \beta u_p} \frac{e^{-A^2}}{\int_{-\infty}^{A} e^{-y^2} dy} \right\} \tag{20}$$

where $A = \dfrac{1 - u_p}{\sigma}$

and $\displaystyle\int_{-\infty}^{A} e^{-y^2} dy = \tfrac{1}{2} \sqrt{\pi} \left| 1 + \text{Erf } A \right|$

In equation (20), u_p is given by (18) even for $u_p > 1$. The effective width σ_h of the ionosphere varies, but after examining several profiles, a value $\sigma_h = 150$km was chosen as a reasonable average and was used for all cases. With σ_h fixed, (20) is a one-parameter formula for the elevation error.

Equation (20) was also tested against the ray-tracing program. To do so, a re-entry trajectory was generated by the NRTPOD (Non Real Time Precision Orbit Determination) program, using

14

a state vector from a recent KREMS test. This trajectory was used as input to the ray-tracing program, which computed by iteration an apparent trajectory for a radar frequency of 155.5 MHz, using one of three different ionospheric profiles taken at Jicamarca, Peru. The apparent range and elevation and the range error were then used in (20) to find δ, which was compared with the elevation error from the ray-tracing program. The same procedure was followed with a satellite trajectory using a pass with a maximum elevation of 81° and minimum range of 800 km. The effective height H of the ionosphere was varied in (20) to find the best fit for each profile and also the sensitivity of the fit to errors in H. The best value of H appeared to be either the peak height of each profile or slightly higher, depending on the asymmetry of the peak. An error ΔH in estimating H produces an error $\Delta \delta$ in δ, where roughly

$$\frac{\Delta \delta}{\delta} \approx - \frac{\Delta H}{H + \frac{1}{2} r_o \sin^2 E_o} \tag{21}$$

Thus the percentage error in δ is less than that of H.

Tables I - VIII show the results for two of the three ionospheric profiles, shown in Figure 4, and both trajectories.[*] Delta EL is the elevation error computed by ray-tracing, and Delta EL2 is δ from equation (20). The relative error is

$$\left| \frac{\Delta EL - \delta}{\Delta EL} \right| .$$

It is seen from Tables I-IV that by choosing H carefully, one can predict the elevation error to within 3% over the whole trajectory. This can be taken as verification of equation (20).

---

[*] The names NORM40 and LOW2-31 simply label the profiles and have no significance.
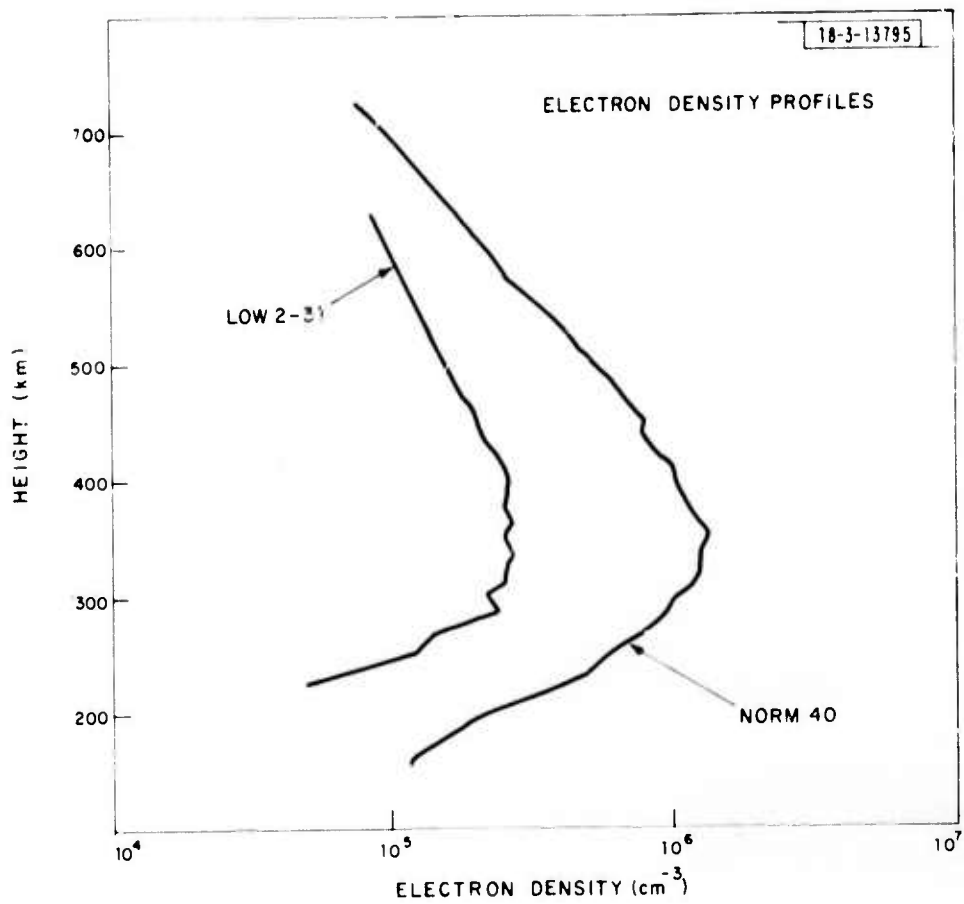
Fig. 4. Ionospheric profiles used to test elevation error formula.

16

TABLE I

TEST OF ELEVATION ERROR FORMULA;

H = 350 km

NORM40   DENSITY   REENTRY   TRAJECTORY   155.50 MHZ

RANGE	DELTA RANGE	ELEVATION	DELTA EL.	DELTA EL.2	RELATIVE ERROR
3674.34	1.7097	0.2219	0.14045	0.13710	0.02338
3520.74	1.7045	1.3635	0.14425	0.14090	0.02323
3364.98	1.6930	2.5011	0.14660	0.14347	0.02135
3207.00	1.6756	3.6350	0.14758	0.14495	0.01846
3046.75	1.6528	4.7654	0.14734	0.14515	0.01485
2884.18	1.6251	5.8931	0.14611	0.14452	0.01088
2719.23	1.5933	7.0183	0.14414	0.14313	0.00696
2551.85	1.5574	8.1415	0.14167	0.14119	0.00341
2381.98	1.5177	9.2627	0.13896	0.13889	0.00060
2209.56	1.4734	10.3820	0.13618	0.13633	0.00107
2034.53	1.4229	11.4990	0.13345	0.13362	0.00128
1856.84	1.3639	12.6130	0.13080	0.13093	0.00012
1676.42	1.2913	13.7218	0.12804	0.12787	0.00138
1493.23	1.1940	14.8221	0.12440	0.12416	0.00192
1307.19	1.0472	15.9059	0.11743	0.11734	0.00078
1118.29	0.8257	16.9589	0.10304	0.10330	0.00251
926.54	0.5058	17.9529	0.07384	0.07393	0.00119
732.26	0.1873	18.8427	0.03438	0.03390	0.01401
536.25	0.0351	19.5094	0.00888	0.00858	0.03455
340.90	0.0010	19.3670	0.00040	0.00040	0.00520

TABLE II

TEST OF ELEVATION ERROR FORMULA;

H = 350 km

NORM40   DENSITY   SATEL   TRAJECTORY   155.50 MHZ

RANGE	DELTA RANGE	ELEVATION	DELTA EL.	DELTA EL2	RELATIVE ERROR
3306.21	1.6979	-0.0839	0.13875	0.13488	0.02793
3118.47	1.6907	1.6412	0.14539	0.14151	0.02670
2930.97	1.6677	3.4753	0.14873	0.14539	0.02243
2743.61	1.6280	5.4406	0.14824	0.14596	0.01540
2556.96	1.5718	7.5663	0.14389	0.14294	0.00661
2371.25	1.5003	9.8905	0.13611	0.13646	0.00259
2186.92	1.4156	12.4637	0.12561	0.12699	0.01099
2004.53	1.3203	15.3533	0.11326	0.11525	0.01751
1824.86	1.2175	18.6496	0.09990	0.10206	0.02166
1648.99	1.1101	22.4765	0.08620	0.08822	0.02343
1478.46	1.0013	27.0039	0.07257	0.07435	0.02306
1315.53	0.8943	32.4654	0.05965	0.06091	0.02109
1163.58	0.7927	39.1729	0.04728	0.04814	0.01825
1027.66	0.7009	47.5058	0.03560	0.03613	0.01499
915.07	0.6245	57.8063	0.02458	0.02488	0.01210
835.44	0.5704	69.9686	0.01427	0.01441	0.00999
798.75	0.5455	81.1651	0.00609	0.00614	0.00900
810.90	0.5539	76.2040	0.00962	0.00971	0.00930
869.83	0.5943	63.6708	0.01936	0.01957	0.01097
966.98	0.6607	52.3434	0.03010	0.03051	0.01352
1092.14	0.7459	43.0395	0.04152	0.04220	0.01661
1236.73	0.8437	35.5547	0.05363	0.05469	0.01973
1394.62	0.9490	29.5036	0.06644	0.06792	0.02220
1561.67	1.0578	24.5351	0.07985	0.08172	0.02339
1735.10	1.1668	20.3767	0.09362	0.09574	0.02265
1913.05	1.2728	16.8286	0.10731	0.10941	0.01958
2094.22	1.3724	13.7453	0.12030	0.12199	0.01405
2277.71	1.4628	11.0207	0.13181	0.13265	0.00636
2462.85	1.5409	8.5769	0.14094	0.14056	0.00268
2649.13	1.6045	6.3554	0.14689	0.14514	0.01191
2836.19	1.6517	4.3124	0.14906	0.14609	0.01993
3023.73	1.6819	2.4142	0.14729	0.14353	0.02552
3211.52	1.6957	0.6356	0.14190	0.13793	0.02801

18

TABLE III

TEST OF ELEVATION ERROR FORMULA;
H = 385 km

LOW2-31 DENSITY   REENTRY TRAJECTORY   155.50 MHZ

RANGE	DELTA RANGE	ELEVATION	DELTA EL.	DELTA EL.2	RELATIVE ERROR
3673.05	0.4174	0.1115	0.03015	0.03025	0.00329
3519.46	0.4160	1.2503	0.03101	0.03111	0.00307
3357.70	0.4131	2.3861	0.03161	0.03172	0.00368
3205.73	0.4087	3.5193	0.03194	0.03209	0.00496
3045.50	0.4029	4.6501	0.03202	0.03222	0.00626
2882.95	0.3956	5.7789	0.03190	0.03214	0.00758
2718.03	0.3870	6.9058	0.03161	0.03187	0.00833
2550.67	0.3768	8.0310	0.03118	0.03144	0.00818
2380.83	0.3650	9.1544	0.03065	0.03085	0.00665
2208.44	0.3512	10.2758	0.03004	0.03014	0.00349
2033.45	0.3349	11.3949	0.02934	0.02930	0.00150
1855.79	0.3150	12.5107	0.02852	0.02830	0.00779
1675.42	0.2903	13.6213	0.02749	0.02711	0.01368
1492.29	0.2594	14.7238	0.02608	0.02566	0.01614
1306.36	0.2187	15.8124	0.02386	0.02354	0.01344
1117.62	0.1626	16.8758	0.01988	0.01972	0.00810
925.13	0.0941	17.8926	0.01345	0.01340	0.00374
772.10	0.0271	18.8131	0.00485	0.00478	0.01316
536.21	0.0030	19.5012	0.00072	0.00071	0.01902
340.80	0.0003	19.3667	0.00008	0.00010	0.22397

19

TABLE IV

TEST OF ELEVATION ERROR FORMULA;

H = 385 km

IONO-31 DENSITY   SATEL   TRAJECTORY   155.50 MHZ

RANGE	DELTA RANGE	ELEVATION	DELTA EL.	DELTA EL.2	RELATIVE ERROR
3304.92	0.4036	-0.1933	0.02943	0.02826	0.01601
3117.18	0.4024	1.5267	0.03093	0.03047	0.01474
2929.60	0.3979	3.3584	0.03184	0.03149	0.01107
2742.37	0.3998	5.3244	0.03204	0.03189	0.00492
2555.76	0.3781	7.4539	0.03149	0.03159	0.00312
2370.11	0.3629	9.7846	0.03020	0.03055	0.01165
2185.85	0.3444	12.3664	0.02830	0.02885	0.01959
2003.53	0.3231	15.2659	0.02591	0.02658	0.02592
1823.94	0.2997	18.5729	0.02320	0.02399	0.02998
1648.15	0.2748	22.4106	0.02031	0.02095	0.03163
1477.71	0.2492	26.9486	0.01735	0.01799	0.03093
1314.86	0.2236	32.4202	0.01442	0.01483	0.02851
1162.99	0.1990	39.1371	0.01155	0.01193	0.02512
1027.13	0.1765	47.4790	0.00877	0.00895	0.02099
914.60	0.1577	57.7878	0.00609	0.00620	0.01739
835.01	0.1442	69.9579	0.00355	0.00360	0.01493
798.34	0.1390	81.1605	0.00152	0.00154	0.01349
810.49	0.1401	76.1568	0.00240	0.00243	0.01402
869.39	0.1501	63.6562	0.00481	0.00489	0.01595
966.49	0.1666	52.3207	0.00744	0.00758	0.01920
1091.58	0.1875	43.0082	0.01018	0.01041	0.02298
1236.10	0.2113	35.5141	0.01302	0.01337	0.02668
1393.91	0.2366	29.4532	0.01595	0.01643	0.02967
1560.87	0.2624	24.4741	0.01893	0.01952	0.03125
1734.22	0.2878	20.3050	0.02188	0.02255	0.03061
1912.09	0.3121	16.7460	0.02471	0.02539	0.02759
2093.19	0.3345	13.6523	0.02727	0.02788	0.02210
2276.60	0.3543	10.9183	0.02943	0.02986	0.01464
2461.68	0.3711	8.4670	0.03101	0.03120	0.00612
2647.91	0.3845	6.2404	0.03189	0.03182	0.00233
2834.94	0.3941	4.1953	0.03201	0.03171	0.00955
3022.45	0.4001	2.2983	0.03138	0.03093	0.01452
3210.22	0.4026	0.5238	0.03010	0.02960	0.01672

20

Tables V-VIII show that if one makes an error of 50km in estimating H, then (20) gives a result correct to within 15% over the entire trajectory. The maximum absolute error of δ in this case is about 0.02^{O} at VHF, compared to a total elevation error of 0.14^{O}. Thus most of the elevation error due to ionospheric refraction can be removed by use of (20), even if the height H is not well known.

E.   Estimation of the Ionospheric Height H

With the width parameter σ fixed in equation (20), four inputs are required by this expression in order to compute elevation error. These inputs are the measured range, elevation, and two-frequency range difference, and the height H. The method of choosing H can be different for real-time vs. post-mission corrections, and may differ for different types of missions. Possible methods include the following:

1.   Set H = 375km (or some other constant average height). The true H is unlikely to be less than 300km or greater than 450km, so the maximum error is roughly 75km, corresponding to an error in δ of less than 25%. This is the simplest solution and probably adequate for real-time estimation.

2.   Make use of a priori knowledge of diurnal and seasonal variations in the height of the ionosphere. Use as input a value consistent with time of day, time of year, location in the sunspot cycle, etc. Tables or curves of the variation of H could be generated.

3.   Use measurements of the ionosphere. If electron density profiles taken just before a mission could be obtained from an ionosonde located at KREMS or at some point near the ground trace of the trajectory, the effective height could be estimated.

4.   Differentiate the range error ΔR. If the look angle (the angle between the target velocity vector and radar line-of-sight)

TABLE V

TEST OF ELEVATION ERROR FORMULA;
H = 435 km Instead of 385 km

LOW2-31 DENSITY   REENTRY TRAJECTORY   155.50 MHZ

RANGE	DELTA RANGE	ELEVATION	DELTA EL.	DELTA EL2	RELATIVE EFFCE
3673.05	0.4174	0.1115	0.03015	0.02667	0.11540
3519.46	0.4160	1.2503	0.03101	0.02744	0.11519
3363.70	0.4131	2.3861	0.03161	0.02801	0.11361
3205.73	0.4087	3.5193	0.03194	0.02839	0.11092
3045.50	0.4029	4.6501	0.03202	0.02858	0.10746
2882.95	0.3956	5.7789	0.03190	0.02860	0.10358
2718.03	0.3870	6.9058	0.03161	0.02846	0.09978
2550.67	0.3768	8.0310	0.03118	0.02817	0.09639
2380.83	0.3650	9.1544	0.03065	0.02777	0.09383
2208.44	0.3512	10.2758	0.03004	0.02727	0.09218
2033.45	0.3349	11.3949	0.02934	0.02666	0.09125
1855.79	0.3150	12.5107	0.02852	0.02596	0.08989
1675.42	0.2903	13.6213	0.02749	0.02513	0.08595
1492.29	0.2594	14.7238	0.02608	0.02408	0.07693
1306.36	0.2187	15.8124	0.02386	0.02236	0.06298
1117.62	0.1626	16.8758	0.01988	0.01891	0.04867
926.13	0.0941	17.8926	0.01345	0.01293	0.03926
732.10	0.0271	18.8131	0.00485	0.00462	0.04597
536.21	0.0030	19.5012	0.00072	0.00068	0.05201
340.80	0.0003	19.3667	0.00008	0.00009	0.17839

TABLE VI

TEST OF ELEVATION ERROR FORMULA;
H = 435 km Instead of 385 km

LCW2-31 CENSITY   SATEL   TRAJECTORY   155.50 MHZ

RANGE	DELTA RANGE	ELEVATION	DELTA EL.	DELTA EL2	RELATIVE ERROR
3304.92	C.4036	-0.1933	0.C2943	0.02553	0.13241
3117.18	C.4024	1.5267	0.03C93	0.C2690	C.13042
2929.60	C.3979	3.3584	0.03184	0.02786	C.12495
2742.37	C.3898	5.3244	0.C3204	0.02834	0.11544
2555.76	C.3781	7.4539	0.C3149	0.02826	0.10257
2370.11	C.3629	9.7846	0.03020	0.02756	0.C8737
2185.85	C.3444	12.3664	0.C2830	0.02628	0.C7115
2003.53	0.3231	15.2659	0.02591	0.02448	0.05519
1823.94	C.2997	18.5729	0.C2320	0.02225	C.C4C67
1648.15	C.2748	22.41C6	0.C2031	0.01973	0.02828
1477.71	C.2492	26.S466	0.C1735	0.C1703	0.C1858
1314.66	C.2236	32.4202	0.01442	0.01425	0.C1143
1162.99	C.1990	39.1371	0.01155	0.01147	0.CC660
1027.13	C.1765	47.479C	0.CC877	0.00874	0.00384
914.60	C.1577	57.7878	0.00609	0.C0608	0.C0237
835.01	C.1442	69.9579	0.00355	0.00355	0.CC168
798.34	0.1380	81.16C5	0.00152	0.00152	0.00161
810.49	0.1401	76.1568	0.C0240	0.00239	0.CC155
869.39	C.1501	63.6562	0.0C481	0.C0480	0.CC195
966.49	C.1666	52.32C7	0.CC744	C.00742	0.C0290
1091.58	0.1875	43.0C82	0.01018	0.01013	0.CC509
1236.10	C.2113	35.5141	0.01302	0.01291	0.CC9C1
1393.91	C.2366	29.4532	0.C1595	0.01571	0.C1506
156C.87	C.2624	24.4741	0.01893	0.01848	0.02360
1734.22	C.2878	2C.3C5C	0.C2188	0.02111	C.03493
1912.C9	C.3121	16.7460	0.02471	0.02350	0.04866
2C93.19	C.3345	13.6523	0.C2727	0.C2552	C.C6426
2276.60	C.3543	1C.S183	0.02943	0.02705	C.C8C71
2461.68	C.3711	8.4670	0.03101	0.02801	0.C9668
2647.91	0.3845	6.2404	0.03189	0.C2836	C.11C85
2834.94	C.3941	4.1953	0.03201	0.02811	C.12205
3C22.45	C.4001	2.2983	0.03138	0.02732	0.12939
3210.22	C.4026	0.5238	0.03010	0.C2611	0.13258

TABLE VII

TEST OF ELEVATION ERROR FORMULA;
H = 400 km Instead of 350 km

NCRM40   DENSITY   REENTRY TRAJECTORY   155.50 MHZ

RANGE	DELTA RANGE	ELEVATION	DELTA EL.	DELTA EL2	RELATIVE ERROR
3674.34	1.7097	0.2219	0.14045	0.11951	0.14912
3520.74	1.7045	1.3635	0.14425	0.12289	0.14803
3364.98	1.6930	2.5011	0.14660	0.12533	0.14511
3207.00	1.6756	3.6350	0.14758	0.12682	0.14062
3046.75	1.6528	4.7654	0.14734	0.12747	0.13486
2884.18	1.6251	5.8931	0.14611	0.12737	0.12824
2719.23	1.5933	7.0183	0.14414	0.12667	0.12117
2551.85	1.5574	8.1415	0.14167	0.12552	0.11405
2381.98	1.5177	9.2627	0.13896	0.12406	0.10724
2209.56	1.4734	10.3820	0.13618	0.12242	0.10105
2034.53	1.4229	11.4990	0.13345	0.12069	0.09556
1856.84	1.3639	12.6130	0.13080	0.11901	0.09010
1676.42	1.2913	13.7218	0.12804	0.11740	0.08309
1493.23	1.1940	14.8221	0.12440	0.11536	0.07265
1307.19	1.0472	15.9059	0.11743	0.11049	0.05911
1118.28	0.8257	16.9589	0.10304	0.09845	0.04457
926.54	0.5058	17.9529	0.07384	0.07104	0.03792
732.26	0.1873	18.8427	0.03438	0.03270	0.04876
536.25	0.0351	19.5094	0.00888	0.00828	0.06817
340.80	0.0010	19.3670	0.00040	0.00039	0.04328

TABLE VIII

TEST OF ELEVATION ERROR FORMULA;
H = 400 km Instead of 350 km

NOFM40   DENSITY   SATEI   TRAJECTORY   155.50 MHZ

RANGE	DELTA RANGE	ELEVATION	DELTA EL.	DELTA EL2	RELATIVE ERROR
3306.21	1.6979	-0.0839	0.13875	0.11757	0.15261
3118.47	1.6907	1.6412	0.14539	0.12349	0.15067
2930.87	1.6677	3.4753	0.14873	0.12727	0.14426
2743.61	1.6280	5.4406	0.14824	0.12847	0.13340
2556.96	1.5718	7.5663	0.14389	0.12679	0.11888
2371.25	1.5003	9.8905	0.13611	0.12222	0.10204
2186.92	1.4156	12.4637	0.12561	0.11502	0.08428
2004.53	1.3203	15.3533	0.11326	0.10567	0.06706
1824.86	1.2175	18.6496	0.09990	0.09476	0.05147
1648.99	1.1101	22.4765	0.08620	0.08291	0.03816
1476.46	1.0013	27.0039	0.07267	0.07068	0.02750
1315.53	0.8943	32.4654	0.05965	0.05849	0.01947
1163.58	0.7927	39.1729	0.04728	0.04663	0.01371
1027.66	0.7009	47.5058	0.03560	0.03524	0.01002
915.07	0.6245	57.8063	0.02458	0.02439	0.00776
835.44	0.5704	69.9686	0.01427	0.01417	0.00656
798.75	0.5455	81.1651	0.00609	0.00605	0.00614
810.90	0.5539	76.2040	0.00962	0.00956	0.00631
869.83	0.5943	63.6708	0.01936	0.01922	0.00701
966.98	0.6607	52.3434	0.03010	0.02984	0.00871
1092.14	0.7459	43.0395	0.04152	0.04103	0.01171
1236.73	0.8437	35.5547	0.05363	0.05275	0.01645
1394.62	0.9490	29.5036	0.06644	0.06489	0.02337
1561.67	1.0578	24.5351	0.07985	0.07723	0.03283
1735.10	1.1668	20.3767	0.09362	0.08941	0.04500
1913.05	1.2728	16.8286	0.10731	0.10091	0.05970
2094.22	1.3724	13.7453	0.12030	0.11111	0.07641
2277.71	1.4628	11.0207	0.13181	0.11939	0.09419
2462.85	1.5409	8.5769	0.14094	0.12520	0.11173
2649.13	1.6045	6.3554	0.14689	0.12815	0.12757
2836.19	1.6517	4.3124	0.14906	0.12816	0.14026
3023.73	1.6819	2.4142	0.14729	0.12539	0.14871
3211.52	1.6957	0.6356	0.14190	0.12027	0.15245

is small, then

$$-\frac{d}{dt} \Delta R \approx X(r)\dot{R}$$

so

$$-\frac{d}{dt}\left\{[-\frac{d}{dt}\Delta R]/\dot{R}\right\} = \dot{X}(r)\dot{R} \qquad (22)$$

Since $N = 0$ at the peak of the profile, the height h at which the derivative (22) changes sign can be taken as an estimate of H. This method applies primarily to post-mission analysis, but also allows correcting a previously used H for the remainder of the re-entry trajectory in real-time.

It is also possible to use the doppler velocity measured at two frequencies to generate an electron density profile from which H can be found. To see this we next consider the effect of the ionosphere on doppler velocity.

5. DOPPLER ERROR

The phase of the radar returned signal, relative to the local oscillator, is

$$\phi = \frac{2\omega}{c} \int_p n\,ds \qquad (23)$$

where $\omega = 2\pi f$. Again retaining $O(X)$ in n, this becomes

$$\phi = \frac{2\omega}{c}\left[R_t - \int_p X(s)\,ds\right]$$

The rate of change of phase is $\dot{\phi} = \frac{d}{dt}\phi$, and the measured doppler velocity is

$$V_D = \frac{c}{2\omega}\dot{\phi}$$

$$= V_t - \frac{d}{dt}\int_p X(s)\,ds \qquad (24)$$

where $V_t = \dot{R}_t$ is the true doppler velocity.

26

Combining (2b) and (24):

$$V_D = V_t - \dot{B}/f^2 \tag{25}$$

If V_D is measured at frequencies f_1 and f_2, then the same argument as used for range gives the doppler error ΔV_1 as

$$\Delta V_1 = V_1 - V_t = g(V_2 - V_1) \tag{26}$$

where g is given by (4).

It should be noticed that if the velocity V is computed by differentiating the range in (2a), the result is

$$V_R = V_t + \dot{B}/f^2 \tag{27}$$

Thus the error in range rate, as measured by time delay, is the negative of the error in coherent doppler. This result could be employed to find the doppler correction using a single radar frequency:

$$\Delta V = \tfrac{1}{2}(V_R - V_D) \tag{28}$$

The doppler correction history $\Delta V(t)$ could also be integrated backward in the post-mission analysis of a re-entry to generate the range correction history $\Delta R(t)$. However, this would require that a hard body be tracked continuously through the ionosphere, and is therefore of limited usefulness. Also, the range rate V_R is generally not as precisely determined as V_D, so that the two-frequency correction (26) is preferable to (28) if available.

6. ELECTRON DENSITY PROFILES

Once the range and doppler errors have been found over an altitude interval, an electron density profile can be computed for that interval. The profile will of course be of electron density along the trajectory, rather than the customary vertical profile.

The total time derivative of the range error is from (1)

$$D_t \, \Delta R = \left| \dot{R} \, \partial_R + \dot{E} \, \partial_E + \dot{A} \, \partial_A + \partial_t \right| \int_0^R X(s) \, ds \qquad (29)$$

where E is elevation, A is azimuth, and $\partial_z = \frac{\partial}{\partial z}$. The partial derivative with respect to time results from secular changes in electron concentration along the ray path. Estimates of the maximum rate of change of columnar electron density, as found from satellite measurements, show that this term can be neglected for the applications considered here. Also, we assume that horizontal gradients of electron density are small compared to vertical gradients, so that the rate of change of ΔR with azimuth can be ignored. Then (29) becomes

$$D_t \Delta R = X(R)\dot{R} + \dot{E} \, \partial_E \int_0^R X(s) \, ds \qquad (30)$$

If X(s) is assumed to be a function of altitude only, we can evaluate the rate of change with elevation by writing

$$X(s, \, E + dE) = X(s + d\rho, \, E)$$

where $d\rho$ is the distance which must be added to s to arrive at the same altitude as that resulting from an increase of dE in E. From Figure 3, we find that

$$d\rho = s \, dE \cot (E + \theta)$$

$$= r_o s \cos E \, dE/(r_o \sin E + s)$$

Thus the derivative becomes

$$\partial_E \int_0^R X(s) \, ds = \int_0^R \lceil X(s + d\rho) - X(s) \rceil \, ds/dE$$

$$= r_o \cos E \int_0^R dX/ds \cdot s/(s + r_o \sin E) \cdot ds$$

28

or

$$\partial_E \int_0^R X(s)\,ds = R \cdot \cot E \left| X/(1 + \beta) - \int_0^1 du\, X(u)/(1 + \beta u)^2 \right| \tag{31}$$

Using equation (16a) for δ, this can be written as

$$\partial_E \int_0^R X(s)\,ds = R/(1 + \beta) \cdot \left| X \cot E - \delta \right|$$

Combining this result with (30) and solving for $X(R)$:

$$\frac{40.2}{f^2} N(R) = \frac{D_t \Delta R + q\delta}{D_t R + q \cot E} \tag{32}$$

with

$$q = R\,\dot{E}/(1+\beta)$$

In (32), the quantity $D_t \Delta R$ can be found from the range error. However, it is preferable to use the error in coherent doppler velocity ΔV_D, as given by (26), if the S/N ratio is sufficient to provide accurate doppler velocities at both frequencies. If this is done, it must be remembered that

$$D_t \Delta R = -\Delta V_D \ .$$

In (32), all quantities except the elevation error δ are measured directly (δ could also be measured if elevation could be measured at two frequencies). Using (20) for δ implies that a peak height H for the ionosphere must be chosen in order to compute the profile. In practice, this can be handled by choosing a nominal H, computing a profile N, and using this profile to determine a revised H. If desired, this process can be continued in an iterative manner to obtain successively more accurate profiles and H-values. Alternatively, if the look angle is small, then $\dot{E}$ is small and (32) can be approximated by

$$\frac{40.2}{f^2} N(h) \approx D_t \Delta R / D_t R \tag{33}$$

29

This result can then be used to generate a first order profile from which an H can be determined for use in (32). The profile then obtained, if not very different from the first order result (33), can be taken as correct.

The terms in (32) were estimated for relative magnitude using the re-entry data from Table I. It was found that at the beginning of the tabulated trajectory ($E < 10^o$), $q\xi$ was comparable to $D_t\triangle R$ and $q \cot E$ to $D_t R$ in size. Later in the trajectory, at altitudes near the peak height H, the ratios were $q\delta/D_t\triangle R \approx 0.06$ and $q \cot E/D_t R \approx 0.18$. This indicates that for a typical re-entry, (33) is not a good approximation at long range, but is fairly good near the peak of the ionosphere. It should therefore provide a good first estimate of H.

Once a sufficiently accurate height H and density profile is found, the width σ_h can also be determined. If $\triangle N$ is the full 3 db width in terms of altitude, then

$$\sigma_h = 0.6 \triangle N$$

is the appropriate value to use in (19). However, if the data are insufficient to generate a reliable profile, then a fixed average value of σ_h (e.g. 150 km) may be used in (19), since errors in σ will have even less effect on δ than errors in H.

7. VALIDATION OF ERROR FORMULAS

The above analysis was applied to a recent mission which contained a long track on a single hard target. The target was tracked from above 700 km height through re-entry by ALTAIR UHF and VHF, and from above 600km through re-entry by ALCOR C-band. The two-frequency formulas were applied to the ALTAIR data to find the VHF range and doppler errors. The range differences were numerically differentiated, reversed in sign, and plotted as a function of height, along with the doppler differences.

The results are shown in Figure 5. The agreement between $-D_t \Delta R$ and ΔV is excellent, and the two plots form a well-defined profile. Since $\dot{R}$ is almost constant over the interval of interest, the profile is proportional to the approximate electron density profile given by (33). Thus Figure 5 was used to obtain a peak height $H = 340$ km. This H was then used in (20) to generate the elevation corrections δ.

The VHF metric data (R, AZ, El) were then tested against the ALCOR data, both with and without the ionospheric corrections. To do so, a least-squares trajectory was fit to the ALCOR data, referred to ALTAIR coordinates, and subtracted from the ALTAIR data. The range and elevation residuals using uncorrected VHF data are shown in Figures 6 and 7. The residuals using ALTAIR data with ionospheric correction are shown in Figures 8 and 9. [*]

As seen in the figures, the range error without correction is as large as 1.7km during the observed part of the trajectory. Applying the correction (3) reduces the maximum error to -19m and the rms error to -10m. Elevation error without correction reaches 0.17°. Using the correction (20) reduces the maximum error to 0.05° and the rms error to 0.021°, which is of the same order as the expected residual elevation error of the ALTAIR system.

These results can be taken as additional validation of the error formulas, and as a demonstration of their application to metric data.

---

[*] In each case, a constant bias of 0.14° has been subtracted from the ALTAIR elevation before plotting. This bias is of unknown origin and is approximately the same on all recent missions. It can be determined by comparison with ALCOR elevation during the portion of a trajectory lying below the ionosphere.
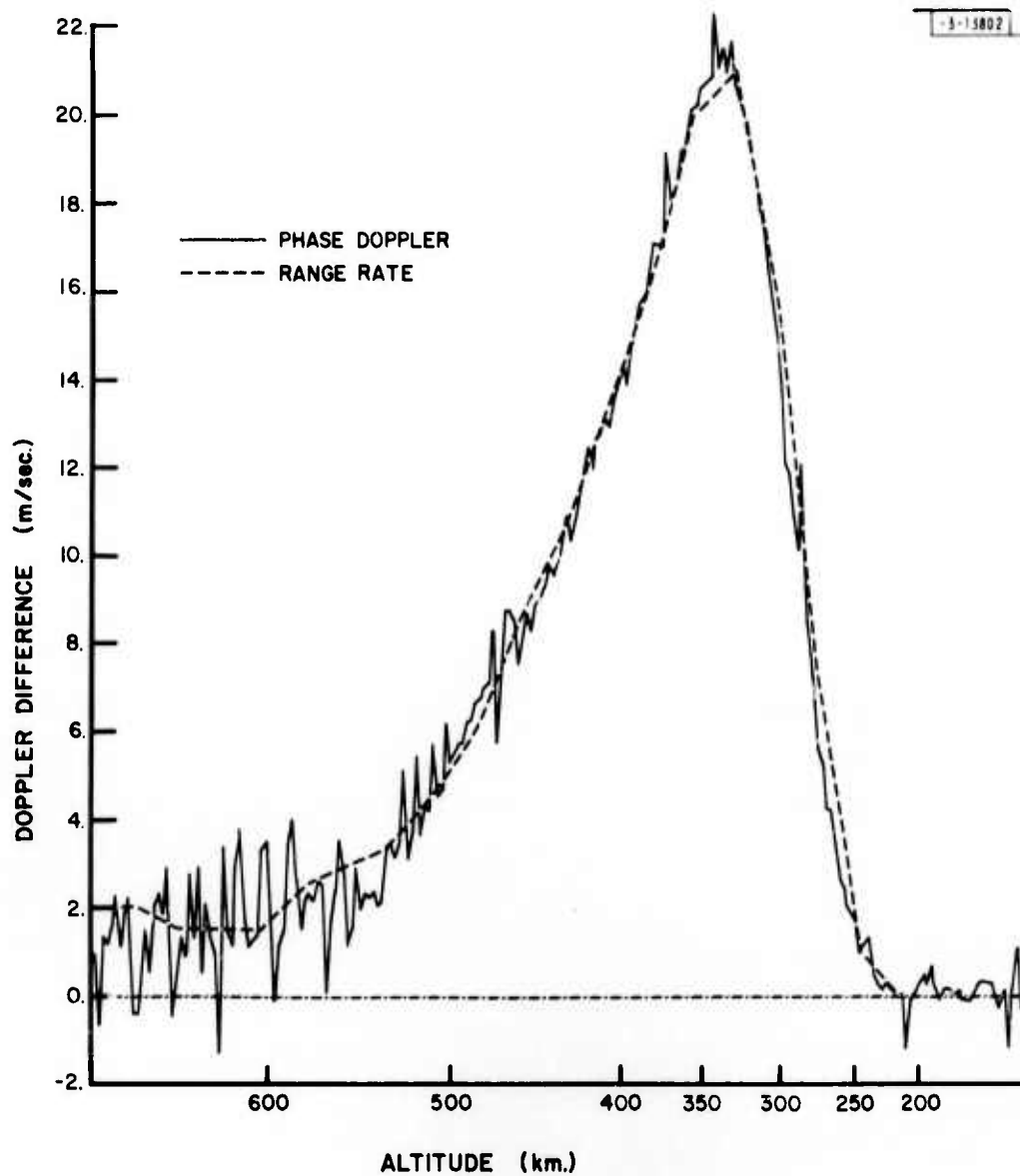
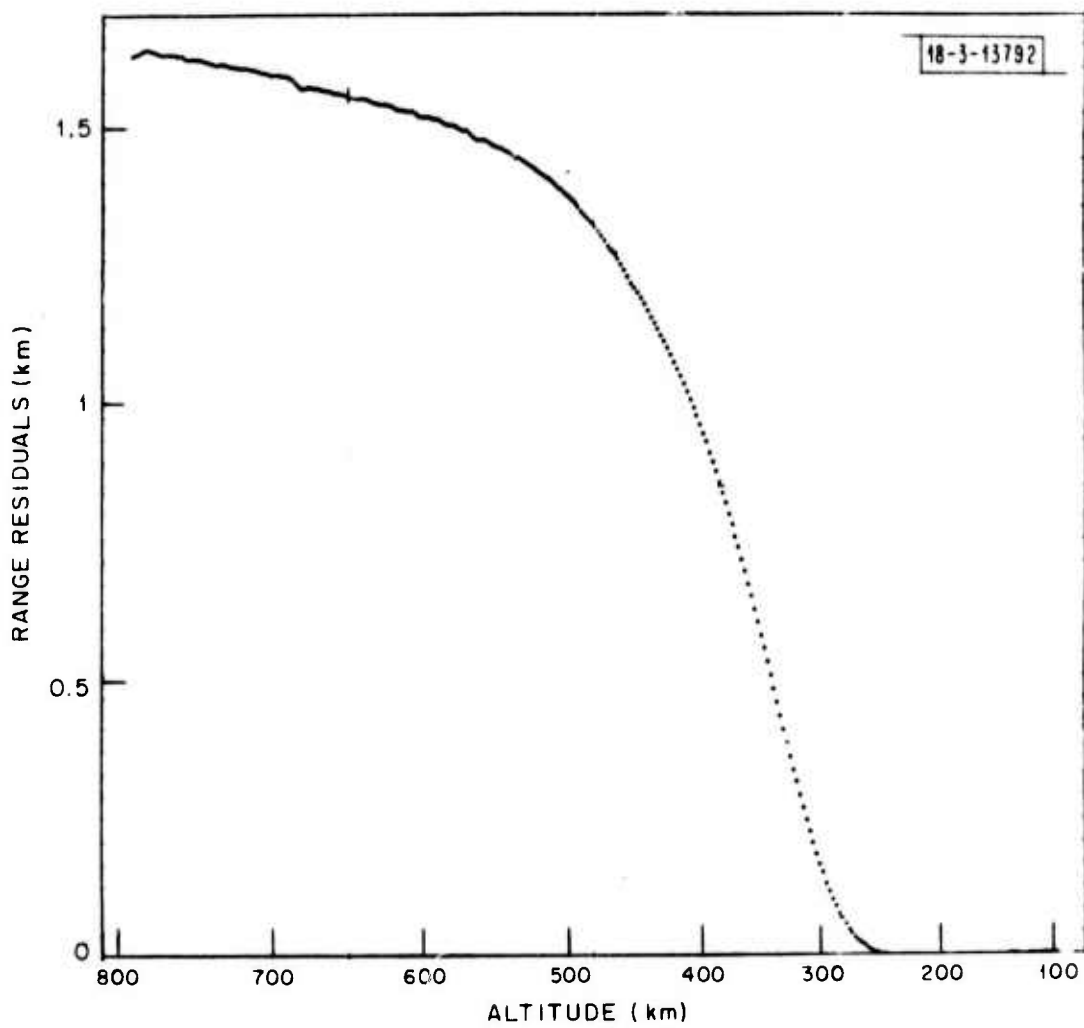Fig. 5. VHF-UHF doppler and range rate differences.

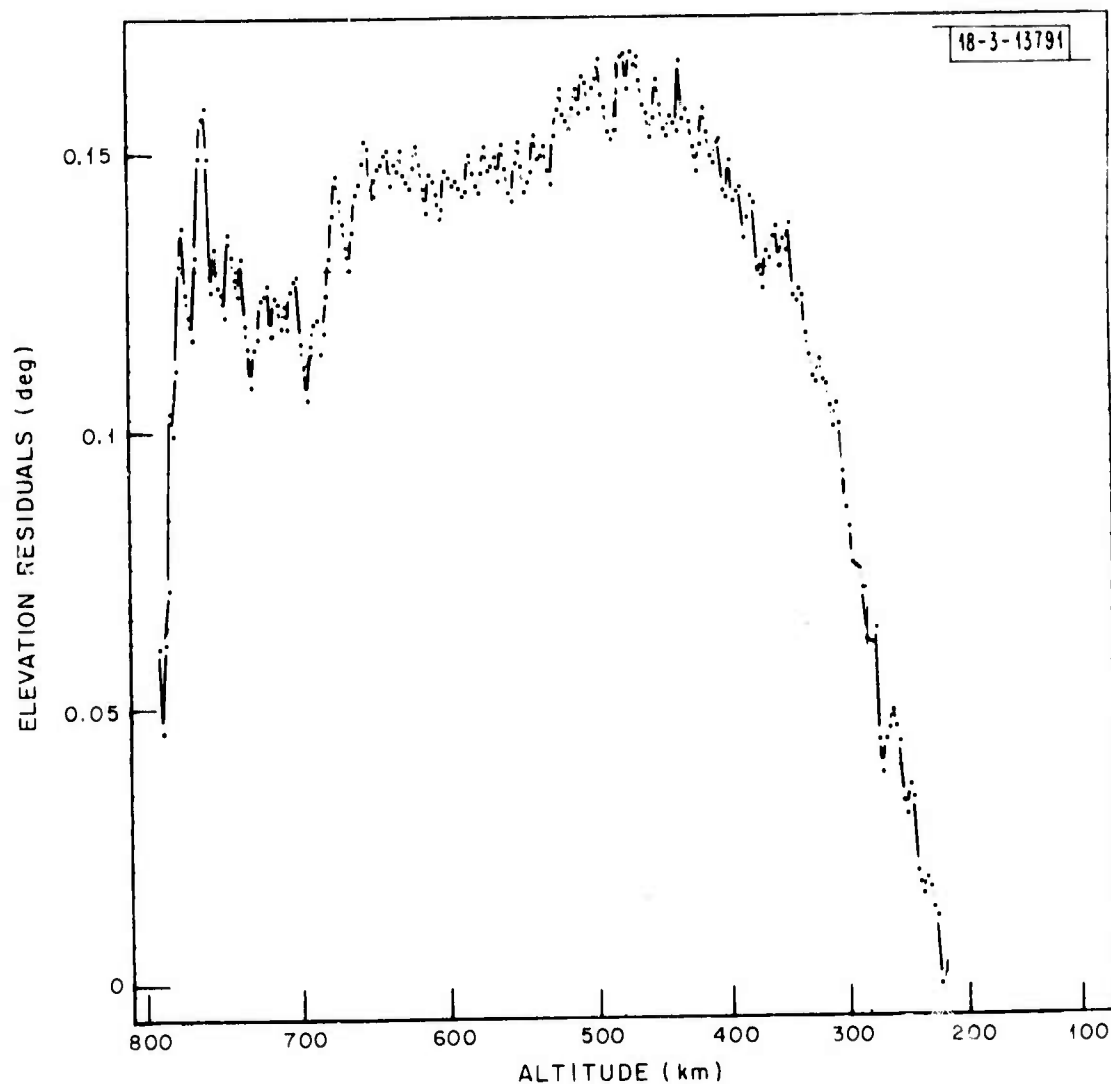Fig. 6.   VHF range residuals without ionospheric correction.

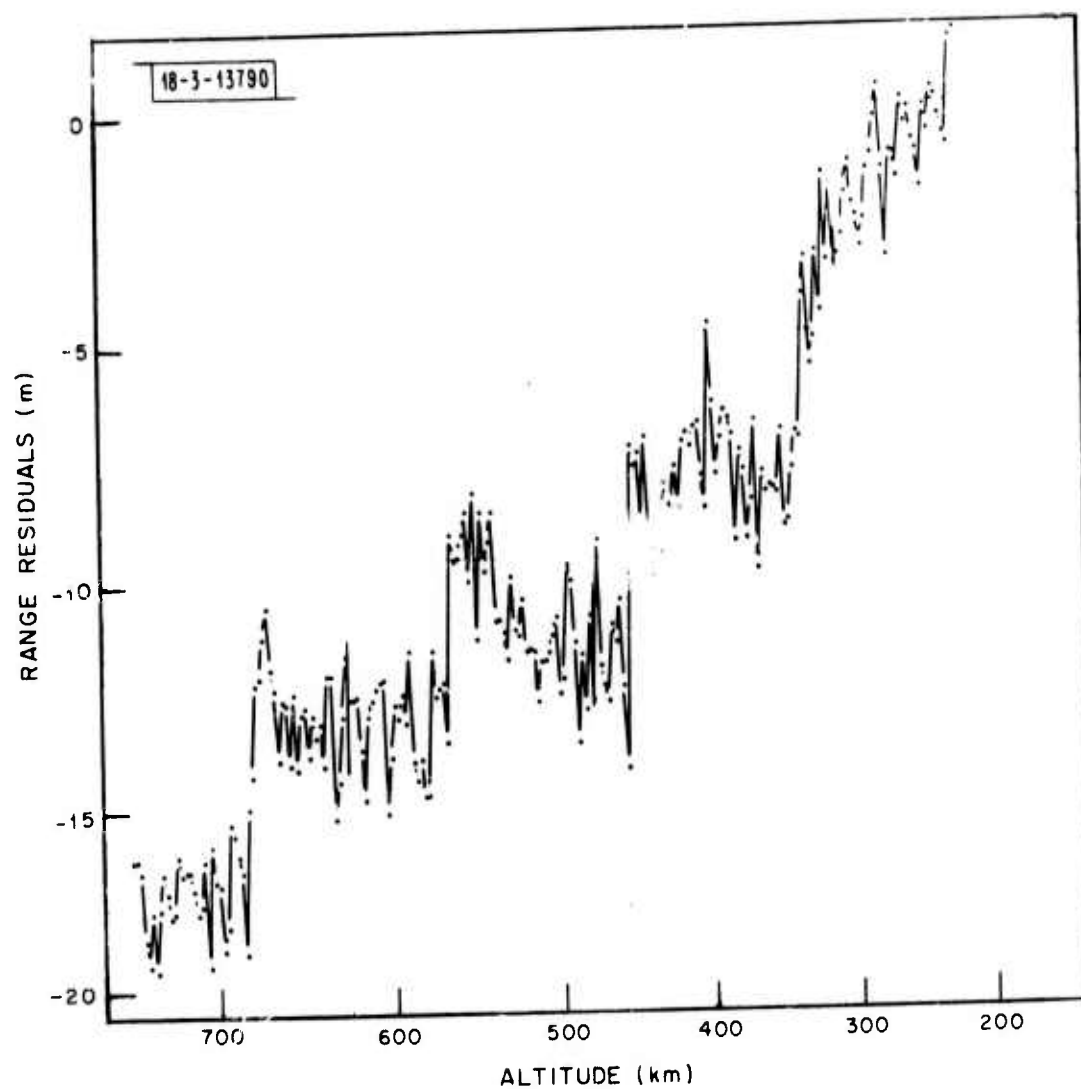Fig. 7.   VHF elevation residuals without ionospheric correction.

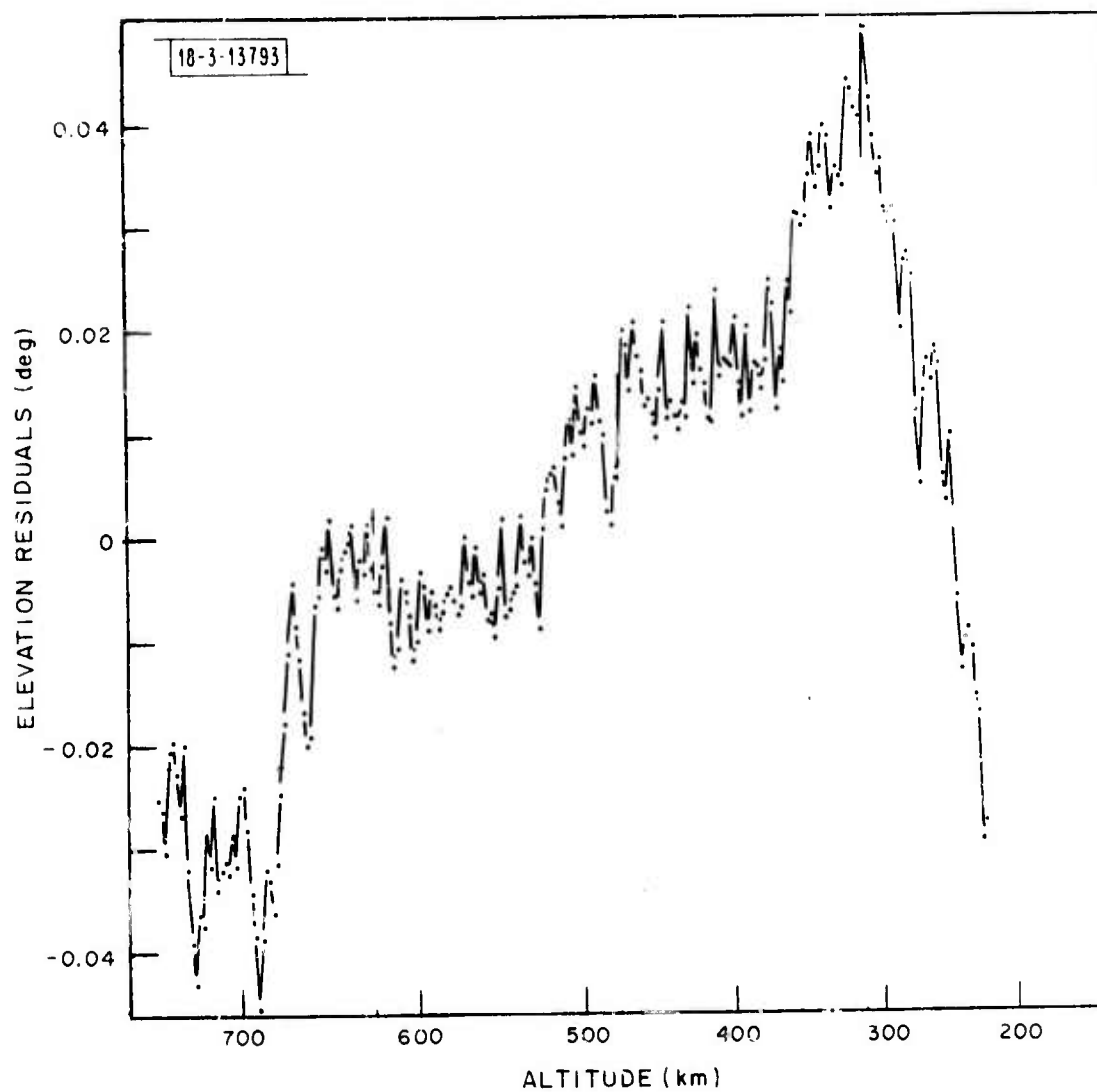Fig. 8.   VHF range residuals with ionospheric correction.

Fig. 9.   VHF elevation residuals with ionospheric correction.

8. FARADAY ROTATION

An additional error in measured metric parameters is caused by the earth's magnetic field. Propagation of a linearly polarized wave in the ionosphere through the earth's field results in a rotation of the plane of polarization of the wave. For the circular polarization transmitted by ALTAIR, the effect can be described by an additional correction in the refractive index:

$$n(s) = 1 - X(s) \cdot \left| 1 \mp \eta\ (s) \right| \tag{34}$$

with

$$\eta = \left| \frac{\omega_B}{\omega} \cos \Phi \right|$$

where

$$\omega_B = \frac{eB}{mc}$$

is the electron gyrofrequency in the earth's magnetic field B, and Φ is the angle between the field and the direction of propagation. In (34) $\eta \ll 1$ has been assumed, along with quasi-longitudinal propagation, which requires that $\Phi - 90^{\circ} > 3^{\circ}$. The upper sign in (34) applies to the ordinary ray and the lower sign to the extraordinary ray.[3]

The range error resulting from (34) is

$$\Delta R = \left| 1 \mp \overline{\eta} \right|\ (\Delta R)_{ion} \tag{35}$$

where

$$\overline{\eta} = \frac{\langle \omega_B \cos \Phi \rangle}{\omega}$$

is an average over the ray path, and $(\Delta R)_{ion}$ is the range error neglecting the earth's field, given by (1).

To estimate the size of this correction at VHF, choose $\omega_B \approx 8 \cdot 10^6$/sec. and $\Phi \approx 60^{\circ}$ for a typical re-entry, so that $\overline{\eta} \approx 0.004$. For propagation northward (along the magnetic field, i.e. $\Phi < 90$), the right circularly polarized beam transmitted by ALTAIR is the extraordinary ray, so that the lower sign in (35)

applies, and the range error due to Faraday rotation is

$$(\Delta R)_B = 0.004 \ (\Delta R)_{ion}$$

For the test data presented above, the maximum $(\Delta R)_{ion}$ is 1.7km, resulting in $(\Delta R)_B \approx 7m$. The largest range error typically seen by ALTAIR is about 3km, corresponding to $(\Delta R)_B \approx 12m$.

Although only right circular polarization is transmitted, both left (principal) and right (orthogonal) circular polarization is received by ALTAIR. The right circular return will show no net magnetic field effect, since the integrated effect along the return path cancels that of the outward path. Thus at a fixed radar frequency, the range error of the principal polarization is larger than that of the orthogonal polarization by the amount $(\Delta R)_B$. Therefore, at VHF, range to a target measured at left circular polarization may be as much as 12m larger than the range measured at right circular for a typical re-entry trajectory. This range difference is a significant percentage of the 30m VHF range resolution. Thus it should be taken into account when detailed comparisons are made of left and right circular data, as in the study of sparse chaff clouds.

Similarly, the earth's field causes a difference in doppler velocity measured at the two polarizations. The difference is $(\Delta V)_B = \pi \ (\Delta V)_{ion}$, and using $\pi = 0.004$ and $(\Delta V)_{ion} \approx 20m/sec$ for the ionospheric error, we find $(\Delta V)_B \approx 0.08m/sec$. Thus the effect of Faraday rotation on doppler velocity can be ignored for most applications. Also, the effect on measured elevation can be neglected, since it is generally no larger than 0.4% of the ionospheric correction given by (20).

Further, it is not necessary to consider the effect when computing range corrections by the two-frequency method. To see this, one recomputes (3) using (34) for the refractive index.

The result is

$$\Delta R_v = (1 + g) [R_v - R_u] \left\{ 1 - \overline{\eta}_v \; \frac{p^2}{1+p} \right\}$$

where g is given by (4) and $p = f_v / f_u \approx 0.375$. Thus the effect of using the refractive index (34) is to change the estimate of the VHF range error by a factor $(1 - 0.102 \, \overline{\eta}_v)$. Again assuming $\overline{\eta}_v = 0.004$ and a maximum value of 3km for ΔR_v, the additional range correction is 1.2m. For the test data presented above, the correction is 0.7m. These values are small compared to the ALTAIR system range residuals and can therefore be neglected.

In summary, the errors in ALTAIR metric data produced by Faraday rotation are negligible when two-frequency measurements are used to correct for ionospheric refraction. However, it is important to consider the effect on range when comparing data taken at principal polarization with that taken at orthogonal polarization.

9. CONCLUSION

The ionospheric corrections described here are currently being employed at Lincoln Laboratory in the analysis of ALTAIR data. As demonstrated in the test data presented here, these corrections have been quite successful in reducing metric residuals, as defined by reference to ALCOR trajectory data. The corrections have also proved helpful in improving impact and pierce point predictions based on exoatmospheric tracks.

The corrections can also be applied in real time, although only the range correction (1) has been used systematically thus far. Adding the elevation correction (20) would result in improved trajectory information for reacquisition and hand-off to other radars.

REFERENCES

1. J. E. Jackson and J. C. Seddon, Journal of Geophys. Res. 63, (1950).

2. R. C. Rose, "A Study of Atmospheric and Ionospheric Re-fraction for VHF, UHF, L-band and C-band Radar Frequencies." PA-158, Lincoln Laboratory, M.I.T., (11 November 1967).

3. G. H. Millman, "Atmospheric Effects on Radio Wave Propa-gation," in R. S. Berkowitz, Modern Radar (Wiley, New York. 1965).

ACKNOWLEDGEMENT